30-SECOND AND ONE-MINUTE RAINFALL RATE MODELLING AND CONVERSION FOR MILLIMETRIC WAVE PROPAGATION IN SOUTH AFRICA

Mary N. Ahuna[1], Thomas J. Afullo[2] and Akintunde A. Alonge[3]

Discipline of Electrical, Electronic and Computer Engineering, University of KwaZulu-Natal, Durban 4041, South Africa
[1]215000279@stu.ukzn.ac.za, [2]afullot@ukzn.ac.za, [3]alongea@ukzn.ac.za

Abstract: The knowledge of adequate rainfall statistics will contribute greatly to the roll-out of emerging wireless technologies on the platform of Long-Term Evolution (LTE) and WiMax (IEEE 802.16). Therefore, it is important that rainfall measurements at shorter integration time are incorporated as useful inputs in the planning of Line-of-Sight (LOS) microwave and millimetre communication links for hosting these technologies. As compared to the use of one-minute rainfall data as suggested by International Telecommunication Union (ITU), the equivalent data measured at 30-second interval gives more information of temporal rain rates in the time domain. Therefore, in this study, rainfall rate measurements of 5-minute integration time representative of 10 locations in South Africa are evaluated to obtain their cumulative distributions. Results from these analyses are compared with rainfall data of one-minute and 30-second integration time data obtained over Durban (29°52'E, 30°55'S), South Africa. Consequently, rainfall rate models for conversion to one-minute and 30-second integration times were obtained over 10 locations in South Africa using the power-law regression functions. Our results obtained over these locations were used to estimate specific attenuation values in selected microwave and millimetric wave bands at 12 GHz, 30 GHz and 60 GHz for 10 locations under study. It is confirmed that the 30-second integration time provides more information needed for estimation of specific attenuation on microwave and millimeter-wave radio links in South Africa.

Key words: Rainfall rate, integration time, rainfall rate conversion factors, specific attenuation

1. INTRODUCTION

Rain-induced attenuation is of great concern to microwave communication system engineers especially at frequencies above 10 GHz [1, 2]. These higher frequencies are utilized by internet service providers (ISPs), online broadcast companies, local multipoint distribution systems (LMDS), as well as satellite networks owing to their high capacity data rate [2, 3]. During the planning, design and implementation of satellite and terrestrial millimetric wave links and systems, sufficient information on rainfall attenuation is required for the location under consideration. This information can be projected by analysing data that has been collected over a period of time over that location, [1–4]. There is a general agreement that rainfall data with lower integration times provides more information for accurate prediction of rainfall attenuation. This is largely due to improved time series resolution of rainfall events which is often necessary to track massive fluctuations in rainfall attenuation. Subsequently, measured data at lower integration times such as one minute or lower become very useful for effective prediction of rainfall effects over radio links at microwave and millimetric wave bands - this information can then be used for effective radio systems design.

Significant research work has been carried out related to rainfall attenuation prediction over South Africa, especially in Durban, for microwave and millimetric wave bands propagation [4-9, 11, 12]. Studies conducted in this region were often centred on seasonal variability of rainfall, rainfall rates and rain drop size distributions. In one of these studies, Odedina and Afullo [7], in their work, suggested rainfall zones for prediction of attenuation based on International Telecommunication Union (ITU) recommendation P.837-4 in [13]. In their work, Odedina and Afullo [7] likewise observed north eastern provinces of South Africa experiences more rain fading compared to the western provinces. Additionally, in his experimental campaign, Owolawi [8] developed rainfall rate contour maps for South Africa's locations for 5-minute to one-minute integration times and this study buttressed the earlier investigations of [7]. Akuon and Afullo [11], using 60-minute and one-minute for Durban, developed conversion factors that could be used by other locations in South Africa to convert their 60-minute data to their equivalent one-minute data. Likewise, [8] developed various rainfall rate conversion methods of Hybrid, Linear, Power and Polynomial functions for conversion of 5-minute data to one-minute integration time over 21 stations in South Africa. Enhancements of rainfall studies were also achieved by rainfall drop size distribution (DSD) approach. In this approach, Alonge

and Afullo [9], with the application of parameter estimation techniques, confirmed that the lognormal and gamma DSDs provided best fits of probability characteristics of drop sizes over Durban. They went further and used this approach to establish seasonal variability of DSDs and their results projected that periods of summer and autumn experience high probabilities of outages in wireless networks over this region. An investigation reveals that overall work done in South Africa has utilized mainly 60-minute and one-minute integration times data [6, 10]. Nevertheless, many researchers have observed that outage prediction analysis for wireless networks require rainfall data with a lower integration time of 30 seconds or less [2, 3, 14]. This observation leads us to undertake this study.

With regard to integration times of less than 60-minute, most research papers have utilized 15-minute, 10-minute and 1-minute data. [3, 8]. Nevertheless, these integration time data are scarce in most parts of the world. Due to this scarcity, radio systems designers may have no option but to estimate rainfall attenuation from processed 60-minute data that is available – though this is not encouraged due to underestimation of rainfall attenuation. It has been observed that better time series of rainfall rate variations are usually obtained from rainfall measurements with less than 60-minute sampling time. Information resulting from these shorter sampling time data is important for radio engineers for determination of sufficient fade margins to overcome rainfall attenuation effects in millimetric wave bands [4, 14]. The main approach for determination of rainfall attenuation for microwaves involves determination of specific attenuation using a power-law function that relates rainfall rate and specific attenuation, [15-17].

National meteorological administrations are indispensable sources of rainfall rate measurements. These administrations archive measured rainfall data that is collected over relatively long periods of time. Alternatively, rainfall rate measurements can also be obtained by carrying out independent measurements using radars, rain gauges or disdrometers with relatively small sampling times [3, 11, 14]. Amongst the three types of measuring instruments, the rain gauge is the most commonly used instrument because it is cost effective and can easily be installed. Different types of rain gauges exist including tipping bucket rain gauges, optical rain gauges, the standard (graduated cylinder) rain gauges, weighing precipitation gauges. When a rain gauge is installed at the surface, it measures the point accumulation of rain-water as rain rate [18].

The Rainfall data collected over Durban was obtained from the disdrometer and the rain gauge over a period of time. These two equipment have varying levels of accuracy and measurement errors, with the disdrometer having an improved sensitivity to rainfall measurements than the rain gauge [18]. The disdrometer unit has two components: outdoor and indoor units. The outdoor unit

consists of a droplet receiving area of 0.005 m². It is capable of processing rainfall data into 20 channels via the indoor unit, [19] with each of the channels related to rain drops with diameter, D_i, in the range $0.3\ mm \leq D_i \leq 5.4\ mm$. The rainfall rate, R, is associated to the mean drop diameter, D_i, in the ith class, by [6, 20]:

$$R = \frac{6\pi \times 10^{-4}}{A \times T} \sum_{i=1}^{20} D_i{}^3 C_i \quad [mm/h] \qquad (1)$$

Where:

C_i = the number of rain drops in the ith class
T = the sampling time given as 60 seconds
$v(D_i)$ = the terminal velocity of rain drop in m/s
A = the sampling area given as 0.005 m²

Conversely, the operation of the tipping rain gauge uses a different measurement principle during measurements of rainfall rates. The tipping sequence is signalled when a reed sensor is triggered. The rain gauge has a poor sensitivity especially at very low rainfall rates (< 2 mm/h), but, on the other hand, it gives a more inexpensive way of collecting rainfall data across the world.

This paper is divided into sub-sections as follows: Section 2 discusses measurements and data processing; in Section 3, we discuss rainfall cumulative distributions and resultant conversion factors generated over Durban; Section 4 presents the application of conversion factors over Durban for generation of conversion factors in other 9 locations of South Africa; Section 5 discusses results associated with specific attenuation and Section 6 provides the conclusion of this study.

2. DATA ACQUISITION

Rainfall data measurements were obtained from the Joss-Waldvögel (JW) RD-80 disdrometer installed at the University of KwaZulu-Natal, Durban, and the rain gauge data obtained from the South African Weather Service (SAWS). Using rainfall data collected over Durban, inferences are made using rainfall rate cumulative distributions in conjunction with their conversion factors. A summary of data measurements are given in Table 1.

Table 1. Rainfall Data Measurements

Integration Time	Duration (Months)
30 seconds	24
1 minute	27
5 minute	132

3.   RAINFALL RATE CUMULATIVE DISTRIBUTION AND CONVERSION FACTORS OVER DURBAN

In this section, analysis of rainfall data measurements at different integration times over Durban are done with the aim of obtaining their cumulative distributions. Furthermore, regression analysis is employed to determine relationships between data at different integration times. For optimal wireless network service in a medium affected by rain, cumulative distributions represents an evaluation technique that can be used to identify the percentage of exceedance probability of rainfall rate. These probabilities enable communication systems design experts to define acceptable fade margin levels required by base stations in the reduction of network outages during rainy periods. Generally, a rainfall rate value corresponding to 0.01% exceedance (or 99.99% rainfall availability), is of major interest for sustainability of satellite and terrestrial communication links. This important parameter is frequently referred to as $R_{0.01}$ and is measured in mm/h. Fig. 1 shows cumulative distributions that are obtained for three categories of rainfall rate integration times over Durban.

3.1   Rainfall cumulative distributions for different integration times over Durban

In Fig. 1 and Table 2, we present cumulative distributions for three different integration times measured over Durban, for rainfall rates exceeded with probability, P, where $0.004\% < P < 9.5\%$. Similarly, in Table 2, a summary of rain rate values at different integration times for percentages of rainfall rates exceeded between 0.01% and 1% are presented. Observations from Fig.1 show that the 30-second cumulative distribution is above the one-minute distribution with a margin of 4.8 mm/h at 99.99% system availability requirement. This is a vital source of information because this part of the graph is the high system availability region that suffers greatly from rainfall attenuation. This further confirms that 30-second integration time data provides more information required for computation of rainfall attenuation compared to one-minute data. It is thus manifested in Fig. 1 that the rainfall rate increases as the integration time decreases. This also confirms that a rainfall rate measuring instrument with a long integration time will not capture shorter peaks present in the high rain intensity, resulting to lower measured rainfall intensities per unit length of time.

As observed from Table 2, it is revealed that R_1 value for 30-second integration time is 6.5 mm/h, $R_{0.1}$ is 24.7 mm/h and $R_{0.01}$ is 64.3 mm/h. For one-minute integration time, corresponding values are 5.8 mm/h, 23.2 mm/h and 59.5 mm/h at 1%, 0.1% and 0.01% probability of rainfall rate exceeded, respectively. For 5-minute integration time, rainfall rates are 3 mm/h, 16.8 mm/h and 55.2 mm/h at the same probabilities of exceedance.

From these results, it is observed that $R_{0.01}$ determined over Durban, though lower for one-minute integration
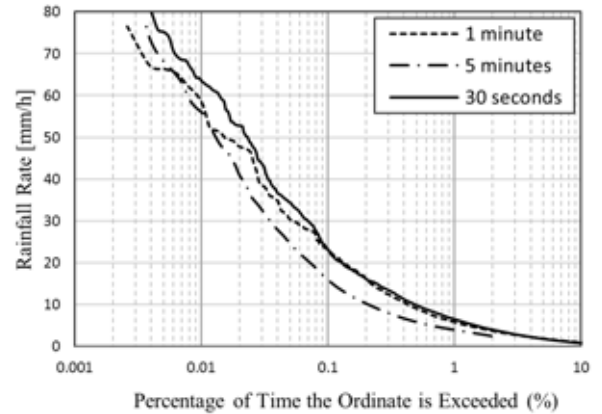

Figure 1: Cumulative distributions from measured rainfall rates for different integration times

Table 2. Measured Rain Rate exceeded for various integration times

Int. Time (sec)	Percentage of time rainfall rate is Exceeded (%)				
	1	0.3	0.1	0.03	0.01
30	6.5	13.6	24.7	43.9	64.3
60	5.8	12.5	23.2	38.3	59.5
300	3.0	8.5	16.8	32.0	55.2

time is comparable to the predicted value of 63 mm/h in ITU-R P.837-1[10] for this region.

3.2   Determination of rainfall rate conversion factors over Durban

Rainfall rate conversion models exist for conversion from higher integration time rainfall rates, $R_{(T\ min)}$, to one-minute integration time rainfall rates, $R_{(1\ min)}$ [8, 14, 21, 22]. This conversion is beneficial in the development of rain rate models that can be applied in the prediction of rainfall attenuation for a given region, [3, 23]. Among existing models, Matricciani [21] proposes a more mathematical approach that aims at resolving errors present in the T-min probability distribution (PD). These errors include upward translation and clockwise rotation of the T-min PD at a fraction of time, $P\%$, where $P > 1$. In this study, we opt to use the power-law relationship method due to its simplicity and ability to provide of useful information in modelling.

A power law relationship relating rainfall rate at the required integration time, τ, and rainfall rate at available integration time, T, at equal probabilities of exceedance, exists. This relationship was established by Ajayi and Ofoche [2], and is given by:

$$R_\tau = u(R_T)^v \quad [mm/h] \qquad (2)$$

Where:

R = the rainfall rate
u = conversion variable
v = conversion variable

Using specialized database of high resolution rainfall data over 47 stations in Canada, Segal, [24] proposed a method of conversion that was expressed as the proportion of equally probable rainfall rates, in the form:

$$\rho_\tau(P) = \frac{R_1(P)}{R_\tau(P)} \qquad (3)$$

and

$$\rho_\tau(P) = aP^b \qquad (4)$$

Where:

$\rho_\tau(P)$ = the conversion factor
$R_1(P)$ = rainfall rate at one-minute integration time
$R_\tau(P)$ = rainfall rate τ-minute integration time
P = equal probability of occurrence
a = regression coefficient
b = regression coefficient

There are two main approaches used for rain rate conversion - use of equivalent rainfall rates or application of the same probability of rainfall rate occurrence [25]. The method adopted in this paper is the equal probability method. Using 5-minute, one-minute and 30-second data collected over Durban, conversion factors for conversion from higher to lower integration times were generated using the power-law fit and are shown in Fig. 2 (a) - (c). Subsequently, these conversion factors are compared to those obtained by other researchers in different parts of the world

Determination of conversion factors for one-minute integration time: Using (2) and regression fitting shown in Fig. 2, one-minute rainfall conversion coefficients as determined for the location of Durban is given in (5) as:

$$R_1 = 1.964\big(R_{5,DBN}\big)^{0.858} \quad [mm/h] \qquad (5)$$

Where:

R_1 = one-minute integration time
R_5 = 5-minute integration time

Results of Table 3 show comparison of regression coefficients u and v obtained over Durban at one-minute integration time with those obtained by Flavin [26] in Australia, USA, Europe and Canada and Ajayi and Ofoche [3] over Ile-Ife in Nigeria. Observations show that the coefficient u in the proposed model for Durban is
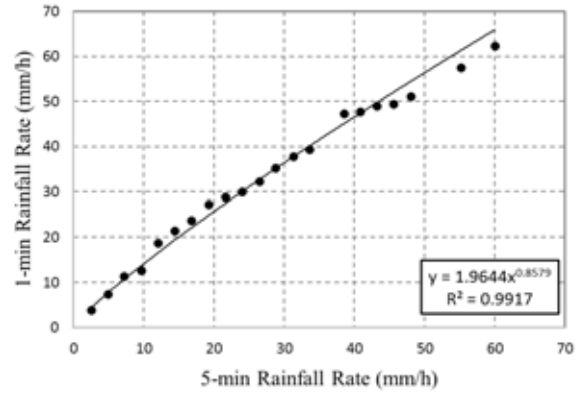

Figure 2: Power-law fits for determination of coefficients u and v for Durban in conversion from 5-minute to one-minute integration time

Table 3. Comparison of Durban's u and v coefficients power-law coefficients with other models

Model	$R_\tau = u(R_T)^v$ for $\tau = 1$ min				Error (%)
	T (min)	u	v	$R_{0.01}$	
AJAYI [3]	5	0.991	1.098	81.0	36.1
OWOLAWI [7]	5	1.062	1.051	71.9	20.8
FLAVIN [25]	6	0.990	1.054	67.9	14.1
Proposed	5	1.964	0.858	61.3	3.0

higher than its counterparts from other locations of the world. From error analysis Ajayi and Ofoche [3] model resulted in an error of 36.1%, the Owolawi [8] model gave error of 20.8%, Flavin [26] model gave 14.1% and the proposed model in (5) produced an error of 3.0%. The highest error is thus observed from Ajayi and Ofoche [3] model. The tropical climate of Ile-Ife, characterized by heavy rainfall may be one factor contributing to this large error, bearing in mind that Durban is mainly subtropical.

From Table 3, it is observed that the Flavin [26] model is closer to the measurements in Durban with an error of 14.1%.

Determination of conversion factors for 30-second integration time: Rainfall rate conversion models from 5-minute and one-minute data to 30-second data were determined using regression fittings in Fig. 3(a) and Fig. 3(b):

$$R_{30s} = 2.078\big(R_{5,DBN}\big)^{0.868} \quad [mm/h] \qquad (6)$$

$$R_{30s} = 1.051\big(R_{1,DBN}\big)^{1.004} \quad [mm/h] \qquad (7)$$

Where:

R_{30s} = the rainfall rate in mm/h at 30-second integration time
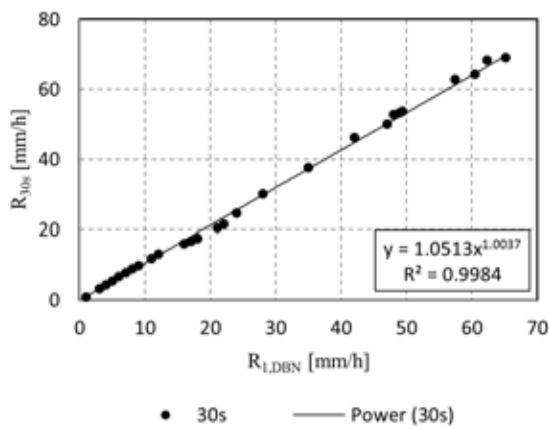R_1 = one-minute integration time rainfall rates

R_5 = 5-minute integration times rainfall rate

It observed from Table 4 that predicted 30-second rainfall rates are higher than measured one-minute and 5-minute rainfall rates and especially at 99.99% system availability requirement. There is a margin of 4.1 mm/h rainfall rate between these two integration times.

Similarly, predicted rainfall rate at 30-second from 5-minute data is 67.6 mm/h, up from a measured value of 55.2 mm/h at 5-minute integration time.
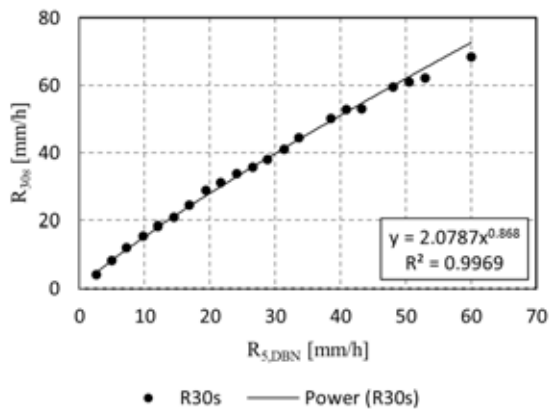
(a)

(b)

Figure 3: Power-law fit for determination of coefficients u and v for Durban in conversion to 30-second from (a) 5-minute (b) one-minute data

Table 4: Predicted rainfall rates at 30-second integration time

Int.Time (T sec)	$R_\tau = u(R_T)^v$ [mm/h], for $\tau = 30$s				
	R_1	$R_{0.3}$	$R_{0.1}$	$R_{0.03}$	$R_{0.01}$
60	6.1	13.3	24.7	40.8	63.6
300	5.4	13.3	24.1	42.1	67.6

3.3 Error analysis and validation of proposed power-law models over Durban

Estimates from our proposed rainfall rate conversion models should be representative of actual measurements. In this regard, our models in (5) - (7) were validated using Root mean Square Error (RMSE) and the Chi squared statistics (χ^2) test for goodness of fit. Expressions that were used for computation of errors are given in (8) and (9) [27]:

$$RMSE = \sqrt{\frac{1}{N}\sum_{k=1}^{k}[y_k - f(x_k)]^2} \qquad (8)$$

$$\chi^2 = \sum_{k=1}^{k}\frac{(y_k - f(x_k))^2}{y_k} \qquad (9)$$

Where:

y_k = measured rainfall rate
$f(x_k)$ = predicted respectively
N = sample size.

In Table 5, we present a summary of results obtained from error analysis in (8) and (9) for power-law models describing our conversion models.

The chi-squared test was carried out at a confidence level of 0.05 and gave values of 2.037, 0.845, and 1.0193, for the three models in (5) - (7), respectively. A comparison with the chi-squared table shows that proposed rainfall rate conversion models passed the test and can be used for future conversions in Durban.

Table 5. Power-Law conversion coefficients for three models over Durban

T (Sec)	$R_\tau = u(R_T)^v$ for $\tau = 60$s			Error analysis	
	u	v	R^2	RMS	CHI
300	1.964	0.858	0.992	1.883	2.037[a]
	$R_\tau = u(R_T)^v$ for $\tau = 30$s				
300	2.078	0.868	0.997	1.324	0.845[b]
60	1.051	1.004	0.998	1.051	1.019[c]

Significant level is given as [a]32.671, at DF = 21, [b]32.671 at DF = 21, and [c]40.113 at DF = 27

Comparisons of proposed models: Durban's one-minute measured rainfall data were compared with selected global models including the Moupfouma and Martin [28] model, the Rice-Holmberg (R-H) [29] model and ITU-R P.837-1[10] model, as shown in Fig. 4. This figure shows
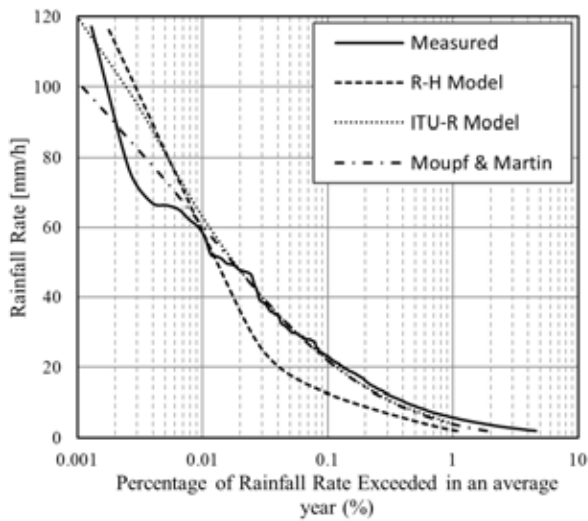
Figure 4: Comparisons of measured and predicted data over Durban with other models

Table 6. Comparison of one-minute Rainfall rates over Durban with other global models

Model	Rainfall rates [mm/h]			RMS (%)
	R_1	$R_{0.1}$	$R_{0.01}$	
Measured (Durban)	5.8	23.1	59.5	-
Moupfouma and Martin	3.9	22.0	59.5	-
R-H Model	2.3	12.6	60.3	1.3
ITU-R Model (Zone M)	4.0	22.0	63.0	5.9

a comparison of measured and predicted rainfall intensities exceeded in a fraction of a year. It is seen from Fig. 4 and Table 6 that the predicted values by other models agree quite well with the measured values. These models predict a rainfall rate of around 60 mm/h at 0.01% exceedance, which is relatively close to proposed $R_{0.01}$ value of 63 mm/h for Durban in region M, [10]. It is also noted that the R-H model overestimates rain rates from 0.004% and below when it is compared with measured values, and this supports Crane's observations that this model overestimates rain rates from 0.01% and lower [14].

Predicted values were compared with the Durban's measured $R_{0.01}$ of 59.5 mm/h and RMS errors show that R-H model is closest to the measured value with an error of 1.3%.

4. DEVELOPMENT OF RAINFALL CONVERSION FACTORS FOR OTHER LOCATIONS IN SOUTH AFRICA

Due to scarcity of, especially one-minute or lower rainfall rates in other locations of South Africa, conversion models developed in (5) and (6) over Durban were used to convert 5-minute rainfall data available in other

Table 7. Geographical description of locations in this study

LOC.	Coordinates		Köppen-Geiger Classification [31]	
	LONGT.	LAT.	Class	Description
BET	28.23ºS	28.30ºE	Cwb	Temperate
BLM	29.12ºS	26.23ºS	Bsk	Steppe
CTN	33.93ºS	18.42ºS	Csc	Temperate
DBN	29.88ºS	31.05ºS	Cfa	Sub-tropical
ELD	32.98ºS	27.87ºS	Cfa	Sub-tropical
IRN	25.87ºS	28.22ºS	Cwb	Temperate
MFK	25.85ºS	25.63ºS	BSh	Steppe
MSB	34.18ºS	22.13ºS	Bsk	Steppe
PLK	23.90ºS	29.45ºS	Bsk	Steppe
UPT	28.40ºS	21.27ºS	BWh	Desert

Key:

Acronym	Name	Acronym	Name
BET -	Bethlehem	IRN -	Irin
BLM -	Bloemfontein	MFK -	Mafikeng
CTN -	Cape Town	MSB -	Mossel Bay
DBN -	Durban	PLK -	Polokwane
ELD -	East London	UPT -	Upington

locations to their equivalent one-minute and 30-second. All geographical locations under study, representing eight out of nine provinces of South Africa, were categorized according to Köppen-Geiger classification as presented in Table 7. Based on earlier research by Köppen and Geiger, [30], the Council for Scientific and Industrial Research (CSIR) created a new Köppen-Geiger classification map for South Africa, [31]. This classification is a 2- or 3-letter code that describes the climatic characteristics of a region by considering a combination of precipitation and temperatures. For instance, a climate described as **Cfa** is a warm temperate climate, fully humid with hot summers and temperatures, $T_{max} \geq +22°C$. A **Csc** is a warm temperate climate with dry and cool summer and cold winter seasons. Winter temperatures drop to as low as -38°C. A **Cwb** climate is warm temperate with dry winter and warm summer seasons with average monthly temperatures of +10°C. The **Bs** code denotes steppe climates with **Bsh** denoting a hot steppe with annual temperatures, $T_{ann} \geq +18°C$. The **BWh** is a hot steppe/desert climate with annual temperatures $T_{ann} \geq +18°C$.

4.1. Empirical distributions for 10 locations in South Africa at 5-minute integration time

Empirical rain rate distributions for different climatic locations within South Africa at 5-minute integration time are presented in Fig. 5. These distributions show probabilities of occurrences of rainfall rate distributions of specified intensities for each location. A summary of measured rainfall rates are summarized in Table 8.
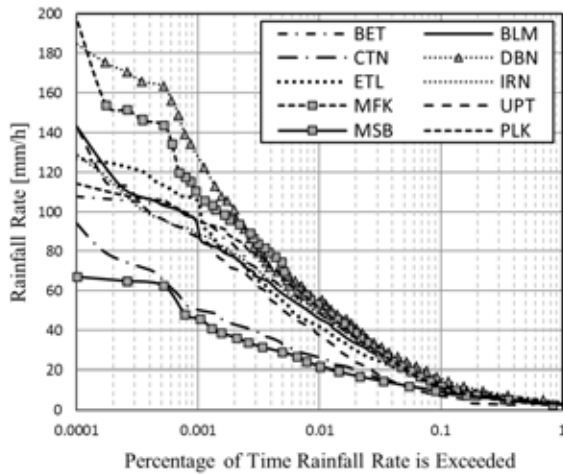
Figure 5: Cumulative distributions for 10 locations at 5-minute integration time

Table 8. Measured Rainfall Rate Intensities at 5-minute Integration Time

Loc.	Rainfall rates [mm/h]				M
	R_1	$R_{0.1}$	$R_{0.01}$	$R_{0.001}$	[mm]
BET	2.5	12.0	48.0	96.0	624.0
BLM	2.5	12.0	45.6	96.0	507.7
CTN	3.0	8.0	26.0	50.5	464.0
DBN	4.0	16.0	55.2	130.0	889.0
ELD	3.5	13.0	41.0	105.0	830.7
IRN	2.8	12.0	48.0	88.0	581.5
MFK	2.3	12.0	52.9	110.4	470.0
MSB	2.7	9.7	21.6	45.6	403.6
PLK	2.6	12.0	51.0	96.0	426.0
UPT	2.1	7.2	36.0	86.4	229.2

As observed in Fig. 5 and Table 8, Durban recorded higher values of rainfall rates exceeded at 0.002% and below compared to other locations, followed by Mafikeng. In the lower end is Mossel Bay and Cape Town with low rainfall rates at the same probability of exceedance. Also, it is observed from Table 8 that there is no obvious correlation between mean annual rainfall and rainfall exceeded for a percentage of time. As an example, East London recorded the second highest annual mean rainfall of 830.7 mm, yet its $R_{0.01}$ rainfall rate was only 41 mm/h as compared with Polokwane's $R_{0.01}$ value of 51.0 mm/h with an annual mean rainfall of 426.0 mm. One explanation for this could be that Polokwane receives heavy rains of convective type within short periods as compared with East London that experiences lighter rains of stratiform type for relatively longer periods. Also, other topographical features, including hills, water masses and presence of mountains, may influence the rain climate of a region.

Observations from Table 8 also affirms Köppen-Geiger classification map for South Africa. For instance, it is observed that Cape Town, with a **Csc** climate, has a

relatively low $R_{0.01}$ rainfall rate of 26.0 mm/h. Cool summers, in this location, experience low amounts of precipitation contributed by less evaporation due to low temperatures. Correspondingly, Durban, classified with a **Cfa** climate, recorded higher rainfall rates of 55.2 mm/h compared with other locations.

4.2. Analysis of rainfall rate conversion factors for other locations in South Africa

Available 5-minute data in 9 other locations in conjunction the 5-minute, one-minute and 30-second data available in Durban, led to development of conversion models for other locations. Following a confirmation drawn from Table 3 that lower integration time data provide more information on rainfall statistics of a location as compared with a higher integration time data, it was deemed necessary to generate conversion factors for other locations to obtain lower integration time data.

Determination of conversion factors for conversion to one-minute integration time: Having obtained useful rain rate values from 5-minute cumulative distributions from selected locations, it is most important to convert these values to values of lower integration as undertaken in [8] and [11]. Akuon and Afullo [11] proposed a mathematical technique of executing this by comparing and substituting the values from rain conversion power-law functions. Firstly, parameters for other locations were determined using the power-law function proposed by [32], [33]:

$$R_1(P) = \mu[R_\tau(P)]^\lambda \qquad [mm/h] \qquad (9)$$

Where:

R_1(P) = one-minute rainfall rates exceeded for a percentage P of the year

R_τ(P) = τ-minute rainfall rates exceeded for a percentage P of the year

μ and λ = regression coefficients.

Making use of (1), conversion factors for Durban were determined as seen in (10),

$$R_{1,DBN} = \mu\left(R_{5,DBN}\right)^\lambda \qquad [mm/h] \qquad (10)$$

Where:

μ and λ = conversion factors obtained for Durban.

The 5-minute equiprobable rainfall rates at each of the 9 locations were used in the determination of regression factors, [11], using (11),

$$R_{5,Y} = \phi\left(R_{5,DBN}\right)^\beta \qquad [mm/h] \qquad (11)$$

Where:

$R_{5,Y}$ = 5-minute equivalent of Durban's 5-minute at region Y

ϕ and β = regression factors for region Y.

Consequently, from (9) - (11), conversion factors from 5-minute data to one-minute data for Location Y in South Africa, can be determined using (12), [11]:

$$R_{1,Y} = \mu \left(\phi \left(R_{5,DBN} \right)^{\beta} \right)^{\lambda} \equiv m \left(R_{5,DBN} \right)^{n} \ [mm/h] \quad (12)$$

Where:

$R_{1,Y}$ = the derived one-minute equivalent rainfall rate for location Y

$\mu, \lambda, \phi, \beta, m$ and n = regression coefficients

and

$$m = \mu \phi^{\lambda} \qquad (13a)$$

$$n = \beta \lambda \qquad (13b)$$

with μ = 1.9644, λ = 0.858 over Durban and values of ϕ and β as given in Table 9.

Consequently, results of the application of the model in (12) to other 9 locations are presented in Table 9.

Determination of conversion factors for conversion from 5-minute to 30-minute integration time: Applying the same concept, used in (10) – (12), a conversion model for conversion from 5-minute data to 30-second data is given as [11]:

$$R_{30s,D} = \phi \left(R_{5,DBN} \right)^{\theta}, \qquad [mm/h] \qquad (14)$$

and,

$$R_{30s,Y} = \varphi \left(\phi \left(R_{5,DBN} \right)^{\beta} \right)^{\theta} \equiv p \left(R_{5,DBN} \right)^{q} [mm/h] (15a)$$

Where:

$R_{30,Y}$ = the equivalent 30-seconds rainfall rates for location Y

p and q = regression coefficients

and

$$p = \varphi \phi^{\theta} \qquad (15b)$$

$$q = \beta \theta \qquad (15c)$$

Table 9. Factors for Conversion from 5-minute data to one-minute data

LOCATION	$R_{5,DBN} \rightarrow R_{5,Y}$		$R_{5,DBN} \rightarrow R_{1,Y}$	
	ϕ	β	m	n
BET	0.910	0.968	1.8117	0.8305
BLM	0.893	0.966	1.7826	0.8288
CTN	0.777	0.875	1.5820	0.7508
ELD	0.970	0.943	1.9137	0.8091
IRN	1.141	0.918	2.1998	0.7876
MFK	0.727	1.057	1.4943	0.9069
MSB	0.951	0.800	1.8815	0.6864
PLK	0.645	1.066	1.3484	0.9146
UPT	0.289	1.191	0.6771	1.0219

Table 10. Conversion factors for conversion from 5-minute data to 30-second data

LOCATION	$R_{30s} = p \left(R_{5,DBN} \right)^{q}$ $[mm/h]$	
	p	q
DBN	2.0780	0.8680
BET	1.9147	0.8402
BLM	1.8836	0.8385
CTN	1.6693	0.7595
ELD	2.0238	0.8185
IRN	2.3301	0.7968
MFK	1.5756	0.9175
MSB	1.9893	0.6944
PLK	1.4202	0.9253
UPT	0.7075	1.0338

with φ = 2.0780, θ = 0.8680 over Durban and values of ϕ and β as given in Table 9 for other locations.

In Table 10, we present conversion factors for different climatic locations in South Africa as processed from 11-year, 5-minute integration time data. From this table, it may be deduced from these coefficients that Durban has higher rainfall rates than other locations under study at the same probability of exceedance.

Rainfall rate cumulative distribution for 10 locations in South Africa: Cumulative distributions over various locations in South Africa at one-minute and 30-second predicted data are presented in Fig. 6 (a) and (b). Observations show that predicted data at 30-second integration time are higher than at one-minute integration time, as expected.

Fig. 6 and Table 11 presents predicted rainfall rates at one-minute and 30-second integration times after application of conversion models in (12) and (15). Observations from this table reveals that rainfall rates at 30-second integration time are higher than those at one-minute integration time at same probability of exceedance. Generally, there is an average margin of 0.95 mm/h at 99% system availability between one-minute and 30-second rainfall rates when all 10 locations
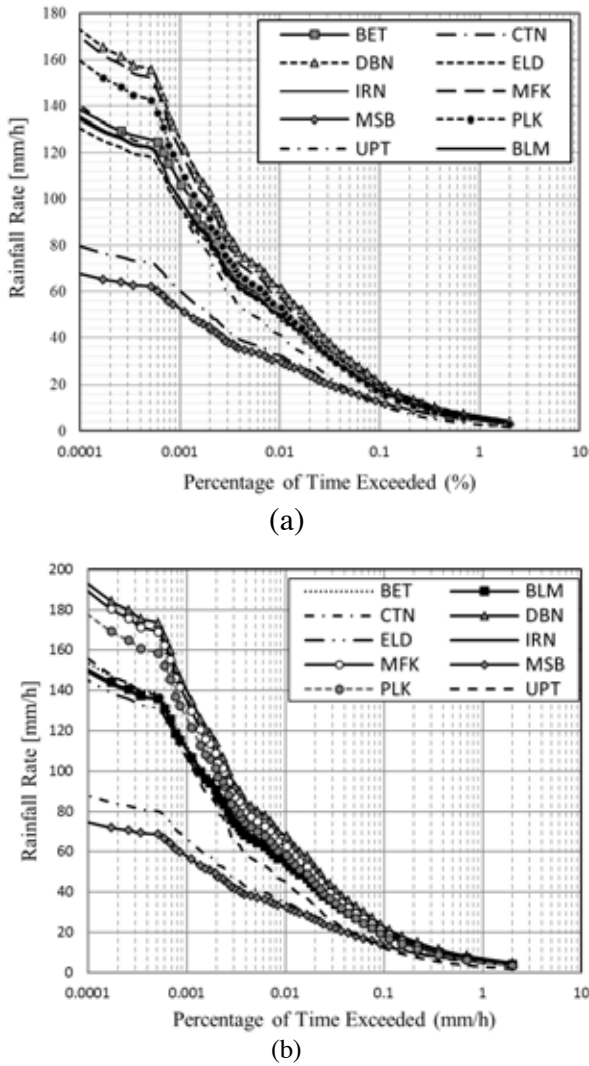
(a)

(b)

Figure 6: Cumulative distributions for 10 locations for predicted rainfall rates at (a) one-minute and (b) 30-second integration times

Table 11. Predicted one-minute and 30-Second Rainfall Rates for 10 Locations in South Africa

Loc.	Rainfall rates [mm/h]					
	$R_{1,Y}$			$R_{30s,Y}$		
	R_1	$R_{0.1}$	$R_{0.01}$	R_1	$R_{0.1}$	$R_{0.01}$
BET	4.5	17.0	50.7	6.3	19.5	55.7
BLM	4.5	16.3	49.5	6.0	19.2	54.4
CTN	3.2	11.7	32.1	4.8	13.6	35.1
DBN	5.8	20.3	61.3	6.8	23.0	67.6
ELD	5.5	17.7	49.1	6.3	19.5	53.9
IRN	5.7	19.2	51.8	7.1	20.1	56.9
MFK	5.6	16.8	56.8	5.8	19.9	62.5
MSB	4.2	11.7	29.5	5.2	13.6	32.2
PLK	5.2	17.8	52.9	5.2	18.4	58.1
UPT	2.8	10.3	40.8	3.0	12.4	44.7

are considered. In the same way, the margins are 2.04 mm/h and 4.66 mm/h at 99.9% and 99.99% system

availability requirements, respectively. The higher margin at high system availability requirement buttresses the need for using rainfall rate measuring equipment with lower integration times for data collection.

Error analysis of proposed power-law models: Owing to lack of measured one-minute data for other locations under study, one-minute predicted values are compared with [34] proposed one-minute rainfall rate exceedance values. Table 12 shows predicted rainfall rate intensities exceeded at one-minute integration time compared to ITU-R P.837-6 proposed valuesfor 0.01% of the average year for each of these locations. The lowest deviation error of -1.0% was observed from the proposed model for Bloemfontein, whereas the highest error of 5.8% is observed in the model proposed for Polokwane. Nevertheless, it is observed that predicted values are comparable to ITU-R values with some slight deviations. This is expected because the empirical measurement analysis gives more accurate values of rainfall intensities for a particular location under study as opposed to regional values that are more generalized. These deviations may be caused by variations in climatic conditions from one location to another within the same region.

5. SPECIFIC ATTENUATION PREDICTION FOR 30-SECOND INTEGRATION TIME OVER SOUTH AFRICA

The fast growing need for high capacity and high speed links for wireless communications is pushing network service providers towards utilization of Ku, Ka and V bands for both terrestrial and satellite communications. Services that need high channel capacity include multipoint video distribution services (MVDS), wireless broadband access (WBA) and other broadband services [1].

The major obstacle in operating at high frequency-bands is signal attenuation caused by electromagnetic wave absorption and scattering in high intensity rainfall rates. An empirical procedure based on the power-law function relating rainfall rate and specific attenuation as proposed by [16] is applied in this section. Specific attenuation values were determined at Ku, Ka and 60 GHz bands as shown in Fig. 7. The 60 GHz channel is an unlicensed band that has been identified for use in short range wireless communications due to its high speed capability and frequency reuse [35]. ITU-R P.838-3 [16] provides a systematic guide in the calculation of specific attenuation, γ_R, for one-minute rainfall on the link as:

$$\gamma_R = kR_1^{\alpha} \; [dB/km] \qquad (16)$$

Where:
R = rain rate in mm/h
k and α = are frequency and polarization dependent coefficients, usually provided by ITU-R P.838-3 [16].

By following the assumption that values of k and α in (16) are wholly frequent-dependent, as deduced in the technical publication of ITU-R P.838-3 [16], it then logically follows from the earlier procedure in (9)-(13) that the equivalent computation of specific attenuation for 30-seconds rainfall rate over any location in South Africa is given as:

$$\gamma_{R,30s} = k(xR_{30}{}^{y})^{\propto} \quad [dB/km] \qquad (17)$$

Where:

x and y = required power-law coefficients for conversion of 30-second rainfall data to one minute as obtained over the investigated locations.

A set of coefficients for three frequencies are given in Table 13. Specific attenuation values were estimated at one-minute integration time at Ku (12 GHz), Ka (30 GHz)

and 60-GHz bands and are presented in Fig. 7 and Table 13 for all locations under study.

Observations from Table 14 indicate that, for instance, there is need to allocate more fade margins for communication links over Durban than Mossel Bay over the same link length. Otherwise, communication links over Durban need to be shorter than those at Mossel Bay at the same frequency. Another observation drawn from this table shows that predicted specific attenuation values using horizontal polarization, are higher than those obtained when using vertical polarization. For instance, there is general average margin of 0.45 dB/km at 12 GHz, 1.56 dB/km at 30 GHz and 1.24 dB/km at 60 GHz for one-minute rainfall at the considered locations in South Africa. However, the trend observed for predictions over 30-second are 0.50 dB/km, 1.76 dB/km and 1.3 dB/km respectively. This suggests that specific attenuation at 30-seconds integration time requires a slightly higher margin to achieve rain fade mitigation at all these locations.

Table 12. Comparison of predicted one-minute $R_{0.01}$ rainfall rates with ITU-R proposed values

Loc.	$R_{1,Y}$	ITU-R	Deviation (%)
BET	50.7	50	1.4
BLM	49.5	50	-1.0
CTN	32.1	30	7.0
DBN	61.3	63	-2.7
ELD	49.1	50	-1.8
IRN	51.8	50	3.6
MFK	56.8	60	-5.3
MSB	29.5	30	-1.7
PLK	52.9	50	5.8
UPT	40.8	40	2.0

Table 13. Frequency-dependent coefficients for estimation of specific rain attenuation as provided by ITU-R [16]

FREQ. (GHz)	k_H	$\propto_H$	k_V	$\propto_V$
12	0.0236	1.1825	0.02455	1.1216
30	0.2403	0.9485	0.2291	0.9129
60	0.8606	0.7656	0.8513	0.7486

Table 13. Frequency-dependent coefficients for estimation of specific rain attenuation as provided by ITU-R [16]

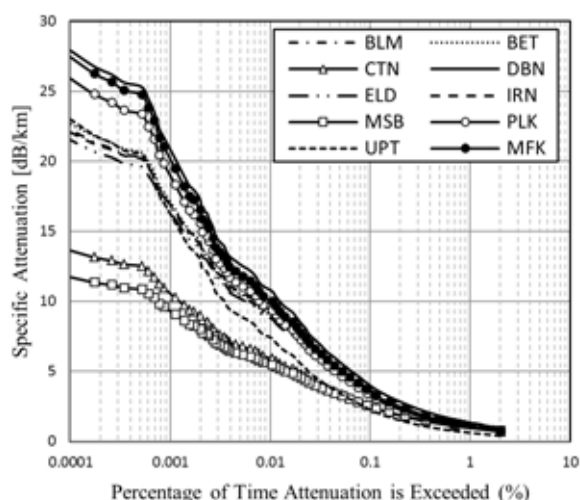| FREQUENCY (GHz)	k_H	$\propto_H$	k_V	$\propto_V$
12	0.0236	1.1825	0.02455	1.1216
30	0.2403	0.9485	0.2291	0.9129
60	0.8606	0.7656	0.8513	0.7486
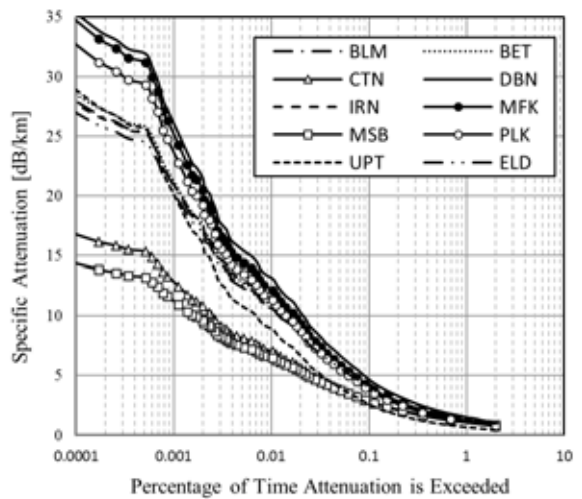
(a)

(b)

Figure 7: Computed specific attenuation exceeded for different percentages of time at one-minute integration time data over South Africa at 30 GHz Band for (a) Horizontal polarization (b) vertical polarization

Also, it is confirmed that specific attenuation due to rainfall increases as frequency of operation increases, as expected. This implies that a consequent increase or decrease in rainfall rate also affects the system availability. As a result, the occurrence of high rainfall rate in Durban will affect the performance of radio links.

6. CONCLUSION

Rainfall rate conversion models for conversion to one-minute and 30-second integration time data for other locations with 5-minute integration time data were developed using available 5-minute, one-minute and 30-second integration time data over Durban. Application of developed conversion models has demonstrated that rainfall rates at lower integration time are comparably higher, providing the much needed information by microwave link designers for the fulfilment of reliable links with optimum availability. Comparison of developed models with other proposed models in other parts of the world showed a general trend of agreement. Measured and predicted one-minute data obtained over Durban were found to be comparable to ITU-R P.837-1 predicted value of 63 mm/h for Durban, South Africa. Specific attenuation values computed based on one-minute and 30 second rainfall rates over South Africa reveal that more fade margins are required for areas that experience higher rainfall rates.

7. REFERENCES

[1] D.L. Emiliani, L. Luini, and C. Capsoni: "Analysis and parameterization of methodologies for the conversion of rain rate cumulative distributions from various integration times to one minute," *IEEE*

Table 14. Predicted Specific Attenuation calculation over South Africa using (16) and (17) at 99.99% system availability requirements

LOC.	$f$req. (GHz)	H_{1min}	H_{30s}	V_{1min}	V_{30s}
BET	12	2.48	2.77	2.01	2.23
	30	9.95	10.9	8.25	8.99
	60	17.4	18.7	16.1	17.3
BLM	12	2.41	2.69	1.95	2.17
	30	9.73	10.6	8.07	8.8
	60	17.1	18.3	15.8	17
CTN	12	1.44	1.6	1.2	1.33
	30	6.45	7.02	5.44	5.9
	60	12.3	13.1	11.4	12.2
DBN	12	3.1	3.47	2.48	2.77
	30	11.9	13.1	9.81	10.7
	60	20.1	21.6	18.5	19.9
ELD	12	2.38	2.67	1.94	2.15
	30	9.65	10.6	8.01	8.74
	60	17	18.2	15.7	16.9
IRN	12	2.54	2.85	2.06	2.29
	30	10.2	11.1	8.41	9.2
	60	17.7	19	16.4	17.6
MFK	12	2.83	3.18	2.28	2.54
	30	11.1	12.2	9.15	10
	60	19.0	20.4	17.5	18.8
MSB	12	1.31	1.45	1.09	1.21
	30	5.95	6.49	5.03	5.47
	60	11.5	12.3	10.7	11.5
PLK	12	2.60	2.92	2.10	2.34
	30	10.4	11.3	8.58	9.36
	60	18.0	19.3	16.6	17.8
UPT	12	1.92	2.14	1.57	1.75
	30	8.10	8.85	6.77	7.37
	60	14.7	15.8	13.7	14.7

Antennas and Propagation Magazine, Vol. 51, No. 3, pp. 70-84, June 2009.

[2] G.O. Ajayi and E.B.C Ofoche: "Some tropical rain rate characteristics at Ile-Ife for microwave and millimeter wave applications," *Journal of Climate and Applied Meteorology*, Vol. 23, pp. 562-567, April 1984.

[3] M.R. UI Islam, T.A Rahman, S.K.A. Rahim, K.F. Al-Tabatabaie and A.Y. Abdulrahman: "Fade margins prediction for broadband fixed wireless access (BFWA) from measurements in tropics,"

Progress In Electromagnetics Research C, Vol. 11, pp. 199-212, 2009.

[4] S.J. Malinga, P.A. Owolawi and T.J.O. Afullo: "Computation of rain attenuation through scattering at microwave and millimeter bands in South Africa," *Progress in Electromagnetics Research Symposium Proceedings*, Taipei, pp. 959-971, 2013.

[5] P.A. Owolawi, T.J. Afullo and S.B. Malinga: "Effect of rainfall on millimeter wavelength radio in Gough and Marion Islands," *Progress in Electromagnetics Research Symposium*, Beijing, China, March 23-27, 2009.

[6] A.A. Alonge and T.J. Afullo: "Seasonal analysis and prediction of rainfall effects in eastern South Africa at Microwave Frequencies," *Progress in Electromagnetics Research B*, Vol. 40, pp. 279-303, 2012.

[7] M.O. Odedina and T.J.O. Afullo: "Characteristics of seasonal attenuation and fading for line-of-sight links in South Africa," *SATNAC*, pp. 1-6, 2008.

[8] P.A. Owolawi: "Derivation of one-minute rain rate from five-minute equivalent for the calculation of rain attenuation in South Africa," *PIERS Online*, Vol. 7, No. 6, pp. 524-535, 2011.

[9] A.A. Alonge and T.J. Afullo: "Regime analysis of rainfall drop-size distribution models for microwave terrestrial networks," *IET Microwave, Antennas and Propagat.*, Vol. 6, No. 4, March 2012.

[10] ITU-R P.837-1 Recommendation, "Characteristics of precipitation for propagation modelling," Geneva, 1994.

[11] P.O. Akuon and T.J.O. Afullo: "Rain cell sizing for the design of high capacity radio link systems in South Africa," *Progress in Electromagnetics Research B*, Vol. 35, pp. 263-285, 2011.

[12] T.J.O. Afullo: "Raindrop size distribution modelling for radio link design along the eastern coast of South Africa," *Progress In Electromagnetics Research B*, Vol. 34, pp. 345-366, 2011.

[13] ITU-R P.837-4 Recommendation: "Characteristics of precipitation for propagation modelling," Geneva, 2003.

[14] R.K. Crane: *Electromagnetic Wave Propagation through Rain*, Wiley Interscience, New York, 1996.

[15] R.L. Olsen, D.V. Rogers, and D.B. Hodge: "The aR^b relation in the calculation of rain attenuation," *IEEE Trans. Antennas Propagat.*, vol. AP-26, pp. 318-329, March. 1978.

[16] ITU-R P.838-3 Recommendation: "Specific attenuation model for use in prediction methods," Geneva, 2005.

[17] M.O. Fashuyi and T.J. Afullo: "Rain attenuation and modelling for line-of-sight links on terrestrial paths in South Africa," *Radio Science*, Vol. 42, RS5006, doi:10.1029/2007RS003618, 2007 pp. 1-15.

[18] J. Wang, B.L. Fisher and D.B. Wolff: "Estimating rain rates from tipping-bucket rain measurements," *Journal of Atmospheric and Oceanic Technology*, pp. 1-45, 2006.

[19] Distromet system: *The Joss-Waldvogel Disdrometer Handbook*, Basel, Switzerland, 2000.

[20] M.J. Bartholomew: "Disdrometer and tipping bucket raingauge handbook," DOE/SC-ARM/TR-079, *ARM Climate Research Facility*, December 2009.

[21] F. Moupfouma: "More about rainfall rates and their prediction for radio systems," *IEEE Proceedings*, Vol. 134 (6), Pt. H, 527-537, 1987.

[22] E. Matricciani: "A mathematical theory of de-integrating long-time integrated rainfall and its application for predicting 1-min rain rate statistics," *International Journal of Satellite Communications and Networking*, 29:501-530, 2011.

[23] B. Segal: "The influence of the raingauge integration time on measured rainfall-intensity distribution functions", *Journal of Atmospheric and Oceanic Technology*, Vol.3, pp. 662-671, December 1986.

[24] C.W. Ooi and J.S. Mandeep: "Empirical methods for converting rainfall rate distribution from several higher integration times into a one-minute integration time in Malaysia," *GEOZIFIKA*, Vol. 30, pp. 143-154, November 2013.

[25] R.K. Flavin: "Rain attenuation considerations for satellite paths," *Telecom Australia Research Laboratories Report*, No. 7505, 1982.

[26] M. Galoie, G. Zenz and A. Motamedi: "Rainfall analysis for the Schoeckelbach Basin (Australia) and determining its best-fit probability distribution model," DOI:10.5675/ICWRER_2013, pp. 43-52.

[27] F. Moupfouma and S. Martin: "Modeling of the rainfall rate cumulative distribution for design of satellite and terrestrial communication systems," *International Journal of Satellite Communication*, Vol. 13, No. 2, pp. 105-115, 1995.

[28] P.L. Rice and N.R. Holmberg: "Cumulative Time Statistics of Surface-Point Rainfall Rates," *IEEE Transactions on Communications*, Vol. COM-21, No. 10, pp. 1131-1136, 1973.

[29] F. Rubel and M. Kottek, "Observed and Projected Climate Shifts 1901-2100 Depicted by World Maps of the Köppen-Geiger Classification," *Meteorologische Zeitschrift*, Vol. 10, No. 2, pp. 135-141, 2010.

[30] D.C.U Conradie: "South Africa's Climatic Zones: Today, Tomorrow," *International Green Building Conference and Exhibition*, Sandton, South Africa, July 2012.

[31] P.A. Watson, M. Gunes: B.A. Potter, V. Sathiaseelan, and J. Leitao, "Development of a climatic map of rainfall attenuation for Europe," Final Report of *ESA/ESTEC* Contract No. 4162/79/NL/DG/(SC), Report 327, 1982.

[32] ITU-R P.837-5 Recommendation: "Characteristics of Precipitation for Propagation Modelling," Geneva, 1994.

[33] ITU-R P.837-6 Recommendation: "Characteristics of Precipitation for Propagation Modelling," Geneva, 2012

[34] N. Guo, R.C. Qui, S.S. Mo and K. Takahashi: "60-GHz Millimeter-Wave Radio: Principle, technology and new results," Research Article, *EURASIP Journal on Wireless Communications and Networking*, Volume 2007, pp. 1-8, December, 2004.